Fatigue Test of MEMS Device : a Monolithic Inkjet Print

Jun-Hyub Park*
Department of Mechatronics Engineering, College of Engineering, Tongmyong University of Information Technology, 535 Yongdang-dong, Nam-gu, Busan 608-711, Korea
Yong Soo Oh
MEMS Lab, Samsung Advanced Institute of Technology, P.O.Box 111, Suwon, Kyongki-Do, 440-600, Korea

A testing system was developed to improve the reliability of printhead and several printheads were tested. We developed a thermally driven monolithic inkjet printhead comprising dome-shaped ink chambers, thin film nozzle guides, and omega-shaped heaters integrated on the top surface of each chamber. To perform a fatigue test of an inkjet printhead, the testing system automatically detects a heating failure using a Wheatstone bridge circuit. Various models were designed and tested to develop a more reliable printhead. Two design parameters of the width of reinforcing layer and heater were investigated in the test. Specially, the reinforcing layer was introduced to improve the fatigue life of printhead. The life-span of heater with a reinforcing layer was longer than that without a reinforcing layer. The wider the heater was, the longer the life of printhead was.

Key Words : Micro-Electro Mechanical Systems (MEMS), Print Head, Fatigue Test, Heater

1. Introduction

A micro-electro mechanical system (MEMS) is a new manufacturing technology for making complex electro-mechanical systems. MEMS uses batch-fabrication processes at a relatively low cost while ensuring the uniformity of a number of repetitive structures. To produce MEMS devices on a commercial scale, however, ensuring their reliability is essential (Tanner et al., 1997; Kolpekwar et al., 1997; Tanner et al., 2000).

Specially, several researchers have studied to improve the life of the thermal ink-jet printhead. Shibata et al. studied on life prolongation of meander-shaped tantalum nitride heating resistors under the condition of a large drive power. They improved the life of heater by placing the meander-shaped heating resistor between SiO_2 layers (Shibata et al., 1989). Aden et al. improved the life of printhead by optimizing the conductor edge profiles (Aden et al., 1989). Chang studied on the effects of alkaline solutions and over-voltage conditions on lifetime and failure mechanisms of thermal ink-jet thin film heater structure (Chang, 1989). Chang et al. studied the effects of the topmost passivation layer in a thermal ink-jet printhead (Chang et al., 1991). Moor et al. found that heaters consisting of sintered and passivated thin Ti/TiN layers have very high reliability (Moor et al., 1999).

The realization of a low-cost and high-resolution inkjet printhead is critical for the future of inkjet printing. An inkjet printhead is classified by its working principle as piezoelectric (Usui, 1996), electrostatic (Kamisuki et al., 2000), and thermal bubble head (Tseng et al., 1998). Due

* Corresponding Author,
E-mail : jhyubpark@korea.com
TEL : +82-51-610-8362; **FAX** : +82-51-610-8349
Department of Mechatronics Engineering, College of Engineering, Tongmyong University of Information Technology, 535 Yongdang-dong, Nam-gu, Busan 608-711, Korea. (Manuscript **Received** August 26, 2003; **Revised** February 15, 2004)

to its low cost and high printing quality, the thermal bubble inkjet printhead has recently dominated the market share, especially of small office and home applications. In a thermal bubble inkjet printhead, a bubble is generated by superheating ink in a chamber ; the rapid growth of the generated bubble ejects an ink droplet out of the chamber.

Currently, two kinds of thermal bubble inkjet printers are commercially available. One operates on the 'sideshooting' principle in which an ink drop is ejected tangentially to the heater surface; the other follows the 'roofshooting' principle in which an ink drop is ejected normally to the heater surface. Samsung Advanced Institute of Technology recently developed its own intrinsic design of a printhead that operates on the backshooting principle (Lee et al., 2001 ; Lee et al., 2001, Maeng et al., 2001 ; Park et al., 2002). In a 'backshooter', recently named by P. Krause and et al.(Krause et al., 1995), a drop is ejected normally to heater while a bubble grows in the opposite direction to the flight of the drop.

With the backshooting principle, the developed printhead enables a monolithic fabrication process that requires no bonding between wafers. The inkjet printhead has a great cost advantage over conventional printheads because of its simpler fabrication process comprising a monolithic process without bonding or assembling nozzle plates. A single cell of the printhead is composed of a dome-shaped ink chamber, a nozzle and nozzle guide, a flow inlet channel and an omega-shaped heater integrated into the roof of each chamber. Its heater is embedded in a thin multilayer in which several materials are deposited. To eject an ink drop, the heater must have a sufficiently high temperature for the ink contacting the surface to instantly reach 280℃. The thin multilayer which has residual stress is then subject to thermal stress and cavitation force caused by the generation and collapse of bubbles. Because the heater in a backshooter printhead was located in the thin roof of each chamber, ensuring its reliability is more difficult than ensuring the reliability of a sideshooter or roofshooter printhead. To assess the reliability of the printhead, we developed a testing system that can test five nozzles simultaneously. The system consists of a PC with a frame grabber card and an A/D and D/A converter, a CCD camera, a microscope, an illuminator, a pulse generator, a relay switch box, and a Wheatstone bridge box with three precision- variation resistors. The system automatically detects a heater failure using the Wheatstone bridge circuit.

To develop a more reliable printhead, we selected two design parameters of the width of reinforcing layer and heater, and tested four types of printhead under the following conditions : 10 kHz frequency, 1 μsec pulse width, and two levels of voltage, 9 and 10 V. Specially, the reinforcing layer was introduced to improve the fatigue life of printhead. It was found that the 12 μm wide heater with reinforcing layer had the longest life at 9 volts. Finally, the wider the width of heater was, the longer the life of heater was and the heater with a reinforcing layer had longer life than that without a reinforcing layer.

2. Design and Fabrication

The monolithic inkjet printhead comprises a dome-shaped chamber with a vertical ink channel, an omega-shaped heater around the nozzle and a thin film nozzle guide, as shown in Fig. 1. Ink is fed to the chamber from the back manifold through the ink channel vertically connected to each ink chamber. The chamber has a dome shape

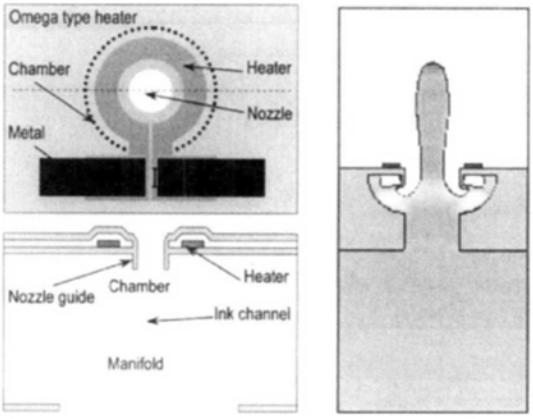

Fig. 1 Schematics of thermal inkjet printhead developed

designed by an isotropic etching technique. A heater is located on top of each chamber and nozzles are placed at the center of the omega-shaped heaters. The structure has a great cost advantage over existing printheads because it uses a simpler fabrication process that comprises a monolithic process without bonding or assembling nozzle plates.

Fig. 2 shows the fabrication process of the monolithic printhead developed. A double-side polished silicon wafer with a (100) surface was used as a substrate. After oxidation (0.25 μm), a pattern was etched on the back of an oxide film by reactive ion etching (RIE) to form a hard mask for silicon anisotropic etching in TMAH solution (a). As a gate material, 0.15 μm thick polysilicon film was deposited in a low-pressure chemical vapor deposition (LPCVD) furnace ; it was then highly doped with phosphorus using a $POCl_3$ source, resulting in resistivity of 50 $\Omega/\square$.

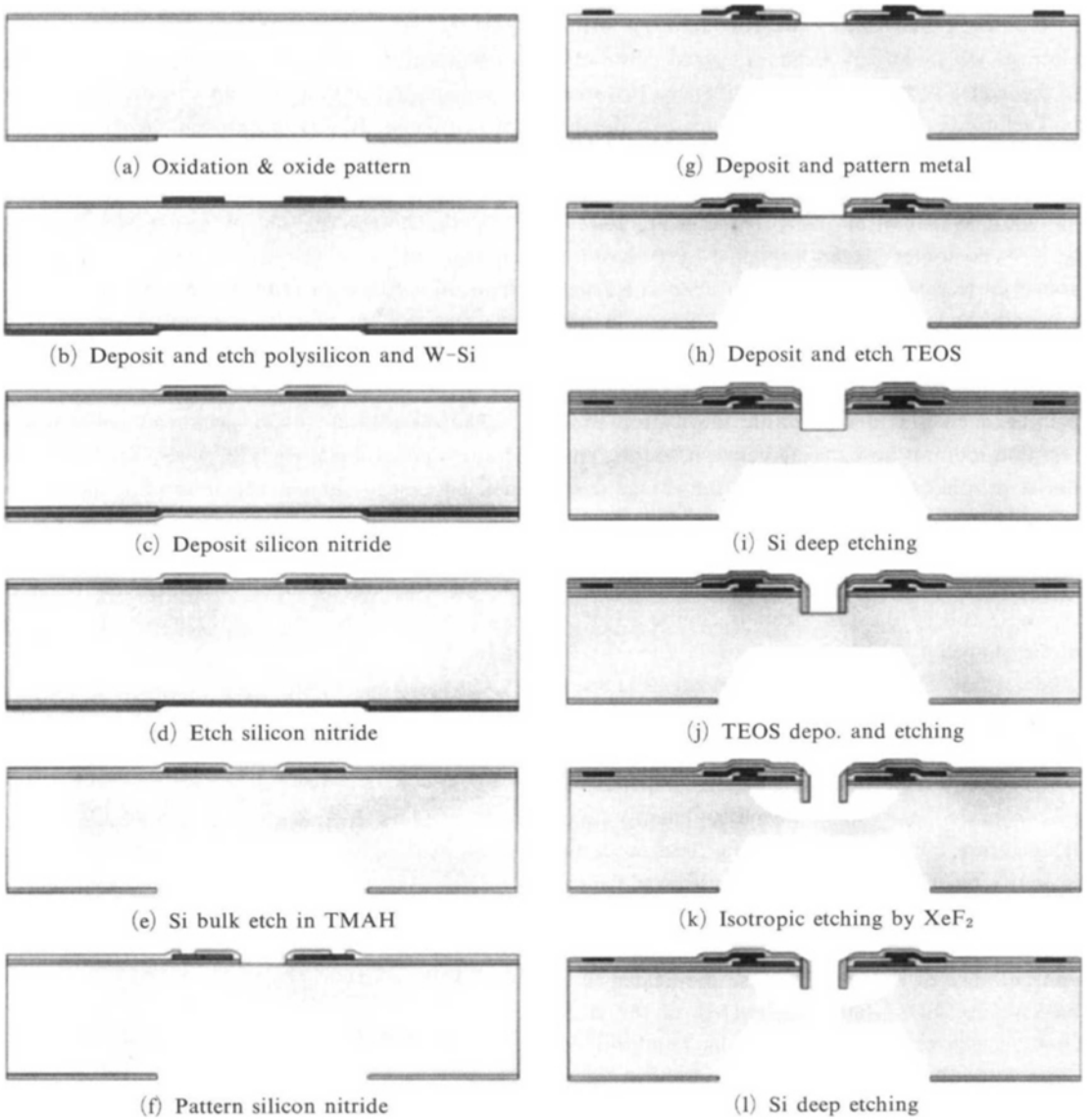

Fig. 2 Fabrication process of inkjet printhead

As a heating material, 0.3 μm thick Tungsten silicide film was deposited and diffused for one hour at 900℃. The polysilicon and Tungsten silicide films were patterned in the shape of the heater for the bubble generation (b). In addition, a silicon nitride film (0.2 μm) was deposited by LPCVD as an insulating material (c). After removal of the silicon nitride and the polysilicon layer from the back of the silicon wafer (d), the silicon substrate was anisotropically etched from the back in 20 wt.% TMAH solution at 90℃, leaving a 50 μm thick silicon membrane after the anisotropic etching (e). Followed by the backside process, a nitride layer was patterned to form a contact window (f). On a patterned nitride layer, a 1 μm thick aluminum film was sputtered and etched into the shape of metal line. This process was followed by an alloying process in a furnace to minimize contact resistance between the aluminum and the Tungsten silicide heater (g). For passivation, a 2.5 μm TEOS oxide film was formed by plasma enhanced chemical vapor deposition (PECVD) and a metal pad was opened by RIE (h). A 0.2 μm LPCVD silicon nitride and 2.5 μm TEOS were deposited for the final stress matching of the nozzle plate released after the formation of the ink chambers. After making a nozzle mask with a photoresist layer, a nitride and oxide film was etched sequentially and silicon was then etched by ICP RIE to form 6 μm high holes (i). To form thin film nozzle guides, TEOS oxide was deposited and anisotropically etched by RIE, leaving the sidewall films inside the nozzle holes (j). To make a dome-shape ink chamber, silicon was isotropically etched in a XeF_2 reactor (k). Finally, the silicon was anisotropically etched by ICP RIE to form vertical ink channels without a photographic step ; the diameter of the channels was the same as the diameter of the nozzles (l). PECVD oxide was deposited with a shadow mask to strengthen the nozzle guide and to make hydrophilic surface inside the chamber and the ink refill channel. In addition, chromium and gold films were introduced at the top surface as an anti-wetting layer.

The fabricated printhead is shown in Fig. 3. The chamber diameter was about 60 μm for the 20 μm nozzle heads, and the thin film nozzle guide was about 6 μm in length. The vertical ink channel was successfully fabricated with the same diameter as a nozzle and a length of about 30 μm. The 56 nozzles were embedded into two columns on each chip, and the pitch between the nozzles was 1/150 inch at each column, as shown in Fig. 4. More than a hundred chips were fabricated on a 100 or 152 mm wafer.

A piece of FPC film was attached to the diced head chip by TAB bonding for an electrical connection to the power supply. The bonded area was encapsulated with an UV curing epoxy and cured at 120℃ for an hour. The bonded device was aligned to an ink bottle and packaged for hermetic sealing. A piece of sponge was then installed inside the bottle to prevent the ink from leaking out of nozzles, and ink was fed to the bottle. Fig. 5 shows the photograph of a packaged printhead.

To choose the printhead with the longest life-span, several printheads were made. Differences

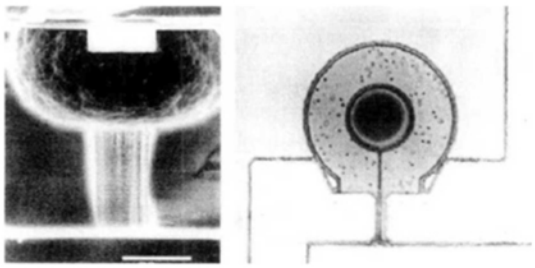

Fig. 3 Photographs of fabricated thermal printhead

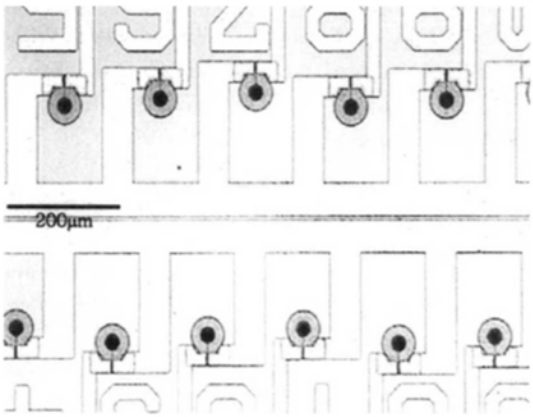

Fig. 4 Chip with an array of 56 nozzles

Table 1 Configuration and dimension of multi-layer (unit : μm)

Type	Configuration of multi-layer					Nozzle guide length	Heater width	Nozzle diameter
	Anti-wetting (Au/Cr)	Heat insulation (Si_3N_4/TEOS/TEOS/SiO_2)	Heater (W-Si)	Heat transfer (P-Si/SiO_2)	Reinforcement (P-Si/W-Si)			
I	0.20/0.02	0.2/0.5/2.0/0.5	0.3	0.15/0.25	0.15/0.3	6	8	20
II	0.20/0.02	0.2/0.5/2.0/0.5	0.3	0.15/0.25	0.15/0.3	6	10	20
III	0.20/0.02	0.2/0.5/2.0/0.5	0.3	0.15/0.25	0.15/0.3	6	12	20
IV	0.20/0.02	0.2/0.5/2.0/0.5	0.3	0.15/0.25	No	6	10	20

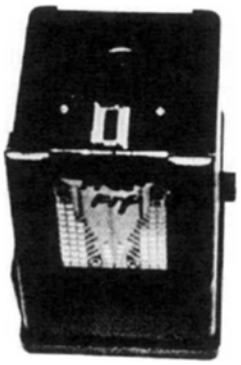

Fig. 5 Photograph of a packaged printhead

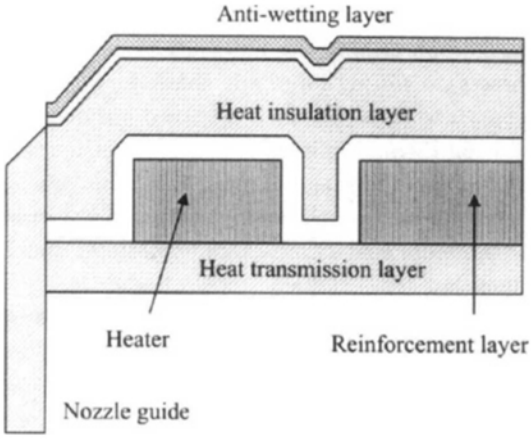

Fig. 6 Section view of multi-layer membrane including heater

in the width of heater and in the stack sequence of membrane are shown in Table 1.

3. Experimental Details

The process of an ink jet printhead is as follows : Ink is fed to a chamber from the back manifold through an inlet ; A voltage pulse with a very short width is applied to a heater. When the temperature of the ink reaches above 280℃, the ink is ejected from the chamber through a nozzle by the generation of a bubble.

The thin multilayer that surrounds the heater was fabricated by depositing several materials. Basically, each layer has inherent and residual stress, and the membrane is subject to thermal stress and cavitation force caused by the generation and collapse of bubbles.

Figure 6 is a sectional view of the multilayer membrane. The membrane is composed of a heater, a heat-transmission layer, a reinforcing layer, a heat-insulation layer and an antiwetting layer. The heat-transmission layer is underneath the heater ; it transmits heat from the heater to the ink without loss of heat. The reinforcing layer is next to the heater on the flat surface of the printhead ; it reinforces membrane. The heat-insulation layer surrounds the upper surface of heater and prevents heat loss when ejecting an ink drop. The antiwetting layer is the most upper layer ; it reduces ink wetting.

To assess a reliability of a printhead, we developed a testing system that can simultaneously test five nozzles. The system consists of a PC with a frame- grabber card and an A/D and D/A converter, a CCD camera, a microscope, an illuminator, a pulse generator, a relay switch box and a Wheatstone bridge box with three precision variation resistors. The system can automatically detect a heater failure using a Wheatstone bridge circuit.

Figure 7 shows a photograph of the system. The block diagram of the system is described in Fig. 8. The block diagram shows the process of ejecting ink and detecting heater failure. A pulse was generated and the pulse passing the Wheatstone bridge circuit generates heat at the heater. The magnitude of the pulse before it passed the Wheatstone bridge circuit was double the magnitude of the pulse after it passed the Wheatstone bridge circuit. We used the Wheatstone bridge circuit to observe the situation of the heater in real time. Fig. 9 shows the Wheatstone bridge circuit, which comprises three precision-variation resistors and the heater to be tested. The life-span of the heater was calculated in two ways. One was to count the TTL signal until the heater failed ; the other was to record the start and end of the heater. If a heater fails, the computer detects the imbalance of the Wheatstone bridge circuit using an A/D converter and sends an interruption signal to the relay switch using the D/A converter. The relay switch then interrupts the input pulse in the heater. To observe the printhead simultaneously, we used a 1/3 inch CCD camera, a microscope and an image-processing system. We developed a program to control the testing system using the commercial software LabView, which is shown in Fig. 10.

To test the reliability of a printhead, we first measured the resistance of the heater and then

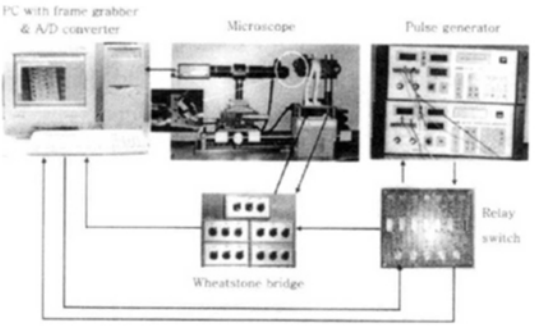

Fig. 7 Photograph of testing system developed

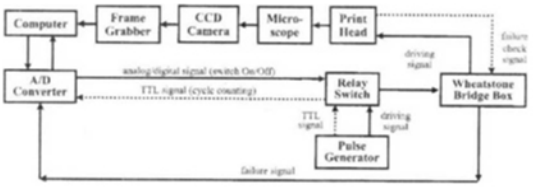

Fig. 8 Schematic diagram of the testing system developed

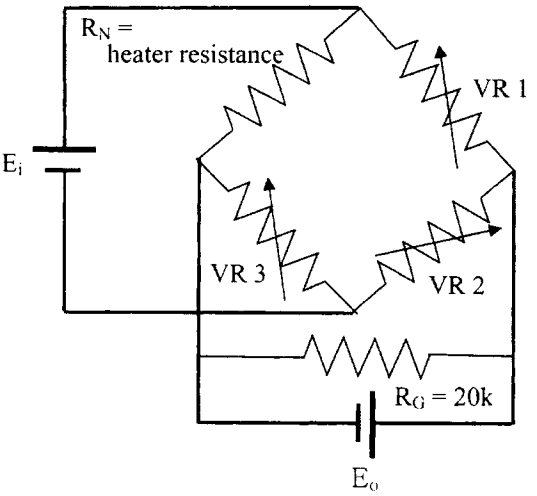

Fig. 9 Wheatstone bridge circuit for detecting failure of heater

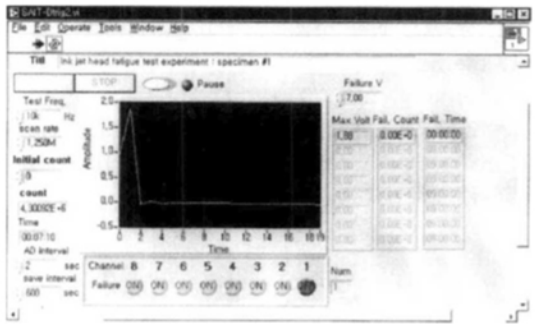

Fig. 10 Screen of the test system developed

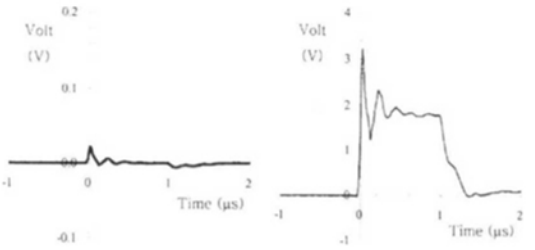

(a) Signal before failing (b) Signal after failing

Fig. 11 Output of wheatstone bridge circuit

balanced the heater and the three precision-variable resistors. In addition, the pulse generator made a pulse with the width and magnitude as shown in Fig. 11. Fig. 11(a) and (b) show the signals passing the Wheatstone bridge circuit before and after heater failure.

To investigate the influence of the width of the heater and reinforcing layer on the life-span of the printhead, we tested the fatigue of the printheads as they eject ink. The frequency of the input signal for testing each heater was 10 kHz and 1 μsec wide pulse. And the driving voltage of pulses supplied to a heater was 9 and 10 volt. While performing the fatigue test, we used a CCD camera to observe the situation of each printhead such as the ejection of ink and wetting. Whenever the printhead was heavily wetted, we cleaned it with tissue moistened by water.

4. Results and Discussion

In this work, we got the test results of Table 2. Two design parameters of the width of reinforcing layer and heater were investigated in the test. The test was performed at two levels, 9 and 10 V. The fatigue tests were performed at the levels satisfying the targets of performances such as velocity and drop volume. Table 2 represents the test conditions, the means and the standard deviations of the results that the 6 samples per a level were tested.

Comparing the test results of Type I, II, and III at 9V, we found that the wider the width of heater was, the longer the life of heater was. Comparing Type II and III with the test results at 9 and 10 V, the life of heater of 12 μm width was about 11 times longer than 10 μm width at 10 V input and the life of heater of 12 μm width was about 2.7 times longer than heater of 10 μm width at 9 V input. Therefore, we found that the wider the width of heater was, the longer the life of heater was, regardless of magnitude of voltage input.

Comparing with the test results of Type II and IV at 9 V and 10 V input to investigate an influence of reinforcing layer, at 9 V input, the life of heater with reinforcing was about 5.3 times longer than heater without reinforcing and at 10 V input, the life of heater with reinforcing layer was also 4.0 times longer than heater without reinforcing layer. Therefore we found that the life of heater with reinforcing layer was longer than heater without reinforcing layer, regardless of magnitude of voltage input.

Figure 12 shows a relationship of voltage input and life. In the figure, x coordinate is logarithm of number of drops to failure of heater and y coordinate is magnitude of voltage input. The line of Type II, heater of 12 μm width and with reinforcing layer is at the most right and the line of Type IV, heater of 10 μm width and without reinforcing layer is at the most left. It means that the life of Type II is longer than Type IV

Table 2 Conditions and results of test

Type	Test condition				Life to failure (drops)	
	Frequency (kHz)	Pulse width (μs)	Heater resistence (Ohm)	Input voltage (V)	Mean	Standard deviation
I	10	1	41.2	9	2.50E+07	2.70E+06
II	10	1	35.2	10	2.52E+06	3.29E+05
	10	1	35.3	9	3.07E+07	3.23E+06
III	10	1	32	10	6.73E+06	4.77E+05
	10	1	32	9	2.74E+08	2.34E+07
IV	10	1	38.1	10	4.76E+05	3.81E+04
	10	1	37.4	9	7.69E+06	3.57E+5

regardless of voltage input.

However, the internal energy per unit volume of heater is important to generate bubble for jetting ink. Such relations between internal energy per unit volume of heater and life are described in Fig. 13. Lines of Type II and III intersect at the point, life=4.09×10^{7} drops and energy=6.97×10^{-3} J/μm^3. Voltage input corresponding to the energy is 9.51 V in Type III and 8.89 V in Type II. Therefore, when energy per unit volume is greater than 6.97×10^{-3} J/μm^3, the heater of 10 μm width, Type II is better than 12 μm width and when vice versa. The figure also shows that heater with reinforcing layer was better than without reinforcing layer.

Figure 14 shows an example of typical failure of heater. Fig. 14(a) is photomicroscope of top surface membrane with heater. The photo indicates that heater failed at opposition to electrode.

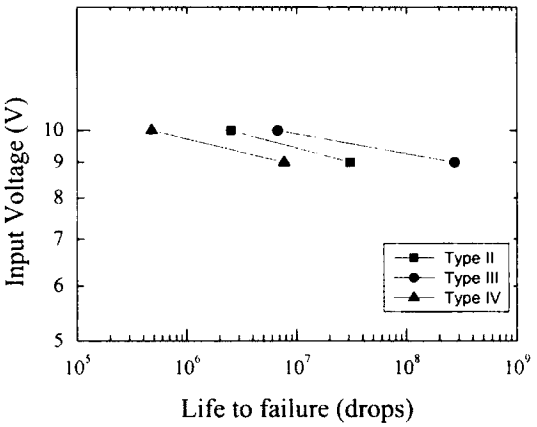

Fig. 12 Relationship between input voltage and life to failure

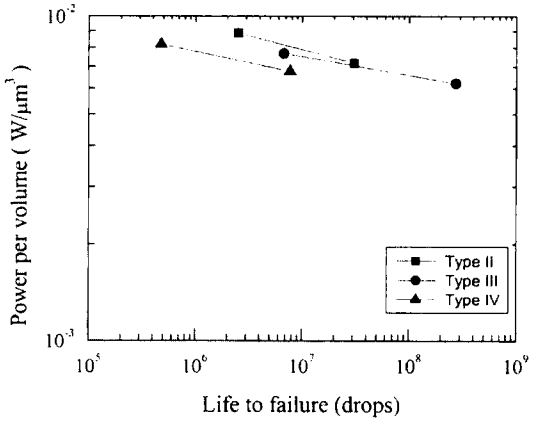

Fig. 13 Relationship between power per volume and life to failure

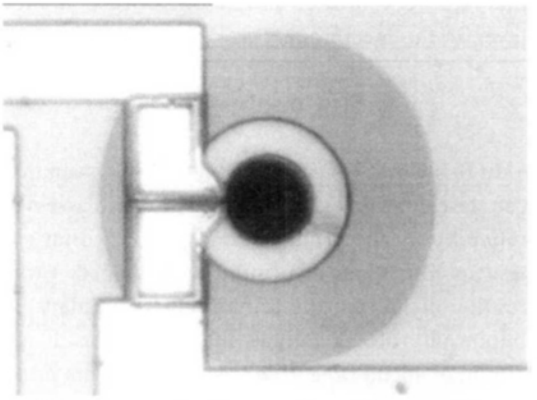

(a) Photograph of top surface of heater failed

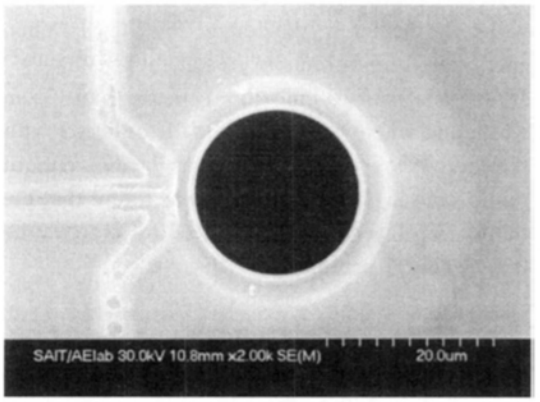

(b) SEM of top surface of heater failed

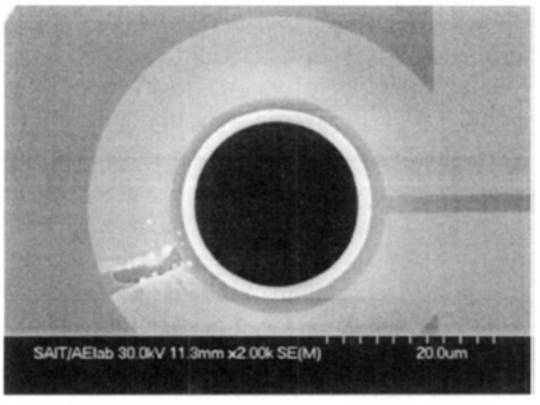

(c) SEM of bottom surface of heater failed

Fig. 14 Photograph and SEM of heater failed

The location is near to where temperature at heater is highest. Fig. 14(b) is SEM of top surface of membrane surrounding heater. We could not see any crack in the SEM. The SEM indicates that the crack is not at top surface of membrane. Although membrane comprises several materials that are very brittle, cracks only occur in one layer of the membrane.

5. Conclusions

In this work, we developed a testing system that can test 5 nozzles, simultaneously, to assess a reliability of the printhead and performed fatigue test for four types of printhead developed. From results of the test, the reinforcing layer plays an important role in fatigue life of printhead and although membrane comprises several materials that are very brittle, cracks only occur in one layer of the membrane. At same voltage input, the wider the heater is, the longer the life is. When energy per unit volume is greater than 6.97×10^{-3} J/μm^3, heater of 10 μm width is better than 12 μm width and when vice versa. The life of heater with reinforcing layer was longer than heater without reinforcing layer. Therefore, it was found that the reinforcing layer to be introduced to improve the fatigue life of printhead is effective.

References

Aden, J. S. and Kahn, J. A., 1989, "Thin Film Device for an Ink Jet Printhead and Process for the Manufacturing," *United States Patent*, Patent No. 4, 809, 428.

Chang, L. S., 1989, "Mechanisms of Failure of Thermal Ink-Jet Thin Film Devices under Stressed Conditions," Proceedings of the SID, Vol. 30/1, pp. 57~63.

Chang, L. S., Gendler, P. L. and Jou, J. H., 1991, "Thermal, Mechanical and Chemical Effects in the Degradation of the Plasma-Deposited α-SiC : H passivation Layer in a Multilayer Thin-Film Device," *Journal of Materials*, Science 26, pp. 1882~1890.

Kamisuki, S., Fujii, M., Takekoshi, T., Tezuka, C. and Atobe, M., 2000, "A High Resolution, Electrostatically-Driven Commercial Inkjet Head," *Proc. of IEEE, The 13th Annual International Workshop on Micro Electro Mechanical Systems*, Miyazaki, Japan, January, pp. 793~798.

Kolpekwar, A. and Blanton, R. D., 1997, "Development of a MEMS Testing Methodology," *Proc. International Test Conference IEEE*, pp. 923~931.

Krause, P., Obermeier, E. and Wehl, W., 1995, "Backshooter-A New Smart Micromachined Single-Chip Inkjet Printhead," *Digest of Technical Papers of The 8th International Conference on Solid-State Sensors and Actuators*, Vol. 2, Stockholm, Sweden, pp. 325~328.

Lee, C. S., Na, K. W., Maeng, D. J., Kuk, K. and Oh, Y. S., 2001, "A Micromachined Monolithic Inkjet Print Head with Dome Shape Chamber," *The 11th International Conference on Solid-State Sensors and Actuators, Transducers'01, Eurosensors XV*, pp. 902~905.

Lee, S. W., Kim, H. C., Kuk, K. and Oh, Y. S., 2001, "A Monolithic Inkjet Print Head : DomeJet," *Technical Digest of 14th IEEE International Conference on Micro Electro Mechanical Systems*, Interlaken, Switzerland, pp. 515~518.

Maeng, D. J., Kuk, K., Lee, C. S., Na, K. W. and Oh, Y. S., 2001, "Performance Improvement in DomeJet Inkjet Print Head by Measuring Temperature of Heater," *The 11th International Conference on Solid-State Sensors and Actuators, Transducers'01, Eurosensors XV*, pp. 910~913.

Moor, P. D., Witvrouw, A., Simons, V. and Wolf, I. D., 1999, "The Fabrication and Reliability Testing of Ti/TiN Heaters," *Part of the SPIE Conference on Micromachining and Microfabrication Process Technology V*, pp. 284~293.

Park, S. J., Kim, M. S., Lee, J. S. and Lee, W. I., 2002, "A Semi-Implicit Method for the Analysis of Two-Dimensional Fluid Flow with Moving Free Surfaces," *KSME International Journal*, Vol. 16, No. 5, pp. 720~731.

Shibata, S., Kanamori, T. and Tsuruoka, T., 1989, "Development of Heating Resistor for Versatile Thermal Print Heads," *IEEE Transactions on Components, Hybrids, and Manufac-*

turing Technology, Vol. 12, No. 13, pp. 358~364.

Tanner, D. M. J., Walraven, A., Helgesen, K., Irwin, L. W., Gregory, D. L., Stake, J. R. and Smith, N. F., 2000, "MEMS Reliability in Vibration Environments," *Proc. 38th Annual International Reliability Physics Symposium*, pp. 139~145.

Tanner, D. M., Smith, N. F., Bowman, D. J., Eaton, W. P. and Peterson, K. A., 1997, "First Reliability Test of a Surface Micromachinned Microengine Using SHiMMeR," *Proceedings SPIE Symposium on Micromachinning and Microfabrication*, Vol. 3224, Austin, pp. 14~23.

Tseng, F., Kim, C. J. and Ho, C., 1998, "A Novel Microinkjector with Virtual Chamber Neck," *Proceedings of IEEE, The 11th Annual International Workshop on Micro Electro Mechanical Systems*, Heidelberg, Germany, January, pp. 57~62.

Usui, M., 1996, "Development of the New MACH," *Proc. of the 12th International Congress on Advances in Non-Impact Printing*, pp. 50~53.